



## Research paper

# An experimental and theoretical kinetic study of the reactions of hydroxyl radicals with tetrahydrofuran and two deuterated tetrahydrofurans

Ádám Illés<sup>a,\*</sup>, Zsófia Borbála Rózsa<sup>b</sup>, Ravikumar Thangaraj<sup>b</sup>, Erzsébet Décsiné Gombos<sup>a</sup>,  
Sándor Dóbe<sup>a</sup>, Binod Raj Giri<sup>c</sup>, Milán Szóri<sup>b,\*</sup>

<sup>a</sup> Institute of Materials and Environmental Chemistry, Research Centre for Natural Sciences, Magyar Tudósok körútja 2, H-1117 Budapest, Hungary

<sup>b</sup> Institute of Chemistry, Faculty of Materials Science and Engineering, University of Miskolc, Egyetemváros 1. A/2 ép. A.1, H-3515 Miskolc, Hungary

<sup>c</sup> King Abdullah University of Science and Technology (KAUST), Clean Combustion Research Center, Division of Physical Sciences and Engineering, Thuwal 23955-6900, Saudi Arabia



## ARTICLE INFO

## Keywords:

Tetrahydrofuran

OH radical

Relative rate experiments

CCSD(T)

Rate coefficient calculations

Kinetic isotope effect

## ABSTRACT

Rate coefficient expressions for the reactions of OH radicals with tetrahydrofuran (THF) (1), 2,2,5,5-tetra-deuterio-tetrahydrofuran (THF-d<sub>4</sub>) (2) and perdeuterated-tetrahydrofuran (THF-d<sub>8</sub>) (3) were determined from relative kinetic experiments over the temperature range  $T = 260\text{--}360$  K displaying a small negative  $T$ -dependence. The following rate coefficients were determined at  $T = 298$  K in  $10^{-11}$  cm<sup>3</sup> molecule<sup>-1</sup> s<sup>-1</sup>:  $k_1 = (1.73 \pm 0.23)$ ,  $k_2 = (0.85 \pm 0.11)$  and  $k_3 = (0.81 \pm 0.12)$ . The experimental  $k(T)$  values agree reasonably well with the high-pressure limit rate coefficients obtained from conventional transition state theory using input data from CCSD(T)/cc-pV(T,Q)Z//MP2/aug-cc-pVDZ computations. Standard enthalpies of formation for THF and two product furanyl radicals were also computed and compared with literature.

## 1. Introduction

Tetrahydrofuran (THF) is a widely used industrial and laboratory solvent and feedstock for the manufacture of polyether polymers, its production amounts to  $\sim 200\,000$  tonnes annually [1]. THF has also become the focus of research interest owing to its potential use as a Cetane Improver [2] and it is considered as a prototype for cyclic bio-fuels [3–7]. Due to the present industrial applications and a possible enhanced future use as a fuel component, an increasing amount of THF gets into the atmosphere inevitably, where it depletes almost exclusively by the reaction with OH radicals [8,9], therefore its atmospheric degradation must be understood.

Several experimental studies have been reported in the literature on the reaction kinetics of OH with THF [10–14]. Ravishankara and Davies [10] and Wallington *et al.* [11] measured rate coefficients for the reaction of OH with THF at room temperature using flash photolysis-resonance fluorescence (FP–RF) technique. Moriarty and co-workers [12] determined Arrhenius parameters by pulsed-laser photolysis experiments coupled to laser-induced fluorescence detection of OH radicals (PLP–LIF) over 263–372 K. They also conducted relative rate measurements using gas-chromatographic analysis (RR–GC). Winer

*et al.* published a rate coefficient at 305 K using a similar relative rate technique [13]. The first combined direct experimental and theoretical kinetic study on the reaction of OH with THF was only disseminated very recently [14]. The CCSD(T)/cc-pV(D,T)Z//MP2/aug-cc-pVDZ-based kinetic results provided excellent agreement with those obtained from shock tube experiments over the temperature range of  $T = 800\text{--}1350$  K. The observed weak temperature-dependence of the overall rate coefficient was captured by the modified Arrhenius expression  $k(T) = (6.82 \cdot 10^{-20}) \times (T/K)^{2.69} \times e^{1316.8K/T}$  cm<sup>3</sup> molecule<sup>-1</sup> s<sup>-1</sup>. The temperature dependent branching fraction of the different H-abstraction channels was also calculated to determine the channel switching between the formation of the radical species tetrahydrofuran-2-yl (THF-R2) and tetrahydrofuran-3-yl (THF-R3). The most recent paper by Fenard *et al.* adopted these rate expressions proposing a detailed model for the combustion of THF evaluated by experimental information from the literature in the temperature range of  $T = 500\text{--}2200$  K [7]. No experiment-based branching fraction of the OH + THF reaction is known from the literature and its direct measurement would be very difficult. On the other hand, kinetic measurement on deuterated THF isotopologues can provide indirect evidence for the site-specific H-abstraction.

\* Corresponding authors.

E-mail addresses: [illes.adam@ttk.hu](mailto:illes.adam@ttk.hu) (Á. Illés), [kemszori@uni-miskolc.hu](mailto:kemszori@uni-miskolc.hu) (M. Szóri).

<https://doi.org/10.1016/j.cplett.2021.138698>

Received 24 September 2019; Received in revised form 22 April 2021; Accepted 26 April 2021

Available online 30 April 2021

0009-2614/© 2021 The Author(s).

Published by Elsevier B.V. This is an open access article under the CC BY-NC-ND license

(<http://creativecommons.org/licenses/by-nc-nd/4.0/>).

Here we report low-temperature rate coefficients ( $T = 260\text{--}360\text{ K}$ ) for the reactions of OH radicals with tetrahydrofuran (THF), 2,2,5,5-tetradeutero-tetrahydrofuran (THF- $d_4$ ) and perdeutero-tetrahydrofuran (THF- $d_8$ ) from relative rate kinetic experiments (RR) and quantum chemistry – reaction rate theory computations for the following reactions:



## 2. Methods

### 2.1. Experimental method

The relative-rate (RR) kinetic experiments [15,16] were performed by comparing the rates of losses of THF and its deuterium isotopologues with that of the reference reactant, diethyl ether (DEE) or cyclohexane (CHX). The reactor was a cylindrical quartz cell of 19.8 cm length and 2.1 cm internal diameter which was equipped with Suprasil windows and temperature-regulated by means of a thermostat allowing the reaction temperature to be kept constant within  $\pm 1\text{ K}$  (errors designate  $2\sigma$  statistical uncertainty throughout the paper). The photolysis cell was fitted with a gas chromatography (GC) sampling port, which included a septum joint and could be evacuated separately from the reactor. OH radicals were produced by the photo-oxidation of methyl nitrite ( $\text{CH}_3\text{ONO}$ ) in synthetic air at atmospheric pressure [15]. The light source was a Xe lamp, the light beam of which was made parallel and passed through an infrared (IR) filter and water filters before entering the reactor through an iris diaphragm [17].

The reaction mixtures contained THF, THF- $d_4$  or THF- $d_8$  in the concentration range  $(0.65\text{--}3.96) \times 10^{16}$  molecules  $\text{cm}^{-3}$ , DEE or CHX reference reactant, 2,2,2-trifluoro-ethanol (TFE) internal GC standard,  $\sim 2 \times 10^{16}$  molecules  $\text{cm}^{-3}$  methyl nitrite and synthetic air close to 1 bar. The gas mixtures were prepared on a vacuum line in a large Pyrex bulb or directly in the cylindrical reactor and the homogeneous mixtures were obtained after at least three hours wait before use under conditions protected from light. All experiments were carried out in  $p = 1100 \pm 100$  mbar synthetic air. The accessible concentration range was limited by the vapour pressure of the reactants and reference compounds at the lowest temperatures of the investigations.

The concentration of the reactants and the reference compound was monitored by temperature-programmed GC using a fused silica capillary column, the GC conditions are given as Supplementary Information (SI) in Table S1. After irradiation, samples for GC analysis were withdrawn by a gastight syringe. 250  $\mu\text{l}$  sample was taken which caused no noticeable reduction of the pressure in the reaction cell. In a test experiment, the reaction mixture was allowed to stand for 48 h in the cylindrical cell in the dark: there was no detectable loss of the chemicals in the gas mixture ( $<2\%$ ) indicating the absence of dark reactions and heterogeneous wall loss. No change of the concentration of the irradiated reaction mixture could be observed in the absence of  $\text{CH}_3\text{ONO}$ .

Synthetic air ( $\geq 99.99\%$ , Messer Hungaria) was used as provided; tetrahydrofuran ( $>99\%$ , Molar Chemicals), perdeutero-tetrahydrofuran ( $>99.5\%$ , Sigma-Aldrich), 2,2,5,5-tetradeutero-tetrahydrofuran (98%, BOC Sciences), diethyl ether ( $\geq 99.8\%$ , Sigma-Aldrich), cyclohexane ( $\geq 99\%$ , Sigma-Aldrich) and 2,2,2-trifluoroethanol (97%, Fluka) were degassed by freeze–pump–thaw cycles prior to use. Methyl nitrite was prepared by dropwise addition of dilute sulphuric acid to a saturated solution of sodium nitrite in aqueous methanol [18] and purified by bulb-to-bulb distillations in vacuum.

### 2.2. Computational method

To extend our knowledge about the reaction mechanism of the H-abstraction reaction of OH radical with THF, the isotope effect was investigated using the zero-point corrected potential energy surface of OH with THF- $d_4$  and THF- $d_8$ . As a starting point, we adopted our previous *ab initio* CCSD(T)/cc-pV(D,T)Z//MP2/aug-cc-pVDZ calculation protocol [14,19,20] which was already used for the reaction of non-deuterated THF and OH [14]. In this protocol, the geometries and harmonic wavenumbers (scaled by a factor of 0.9615 [21]) were obtained at the MP2/aug-cc-pVDZ level of theory [22–24] using the ‘tight’ convergence criterion of the Gaussian09 program package [25]. Then, CCSD(T) complete basis set limit was approximated as a sum of Hartree Fock (HF) limits using cc-pVXZ basis sets ( $X = \text{D, T and Q}$ ) [23] as recommended by Feller [26] and the extrapolated correlation energy as suggested by Helgaker and Klopper [27] using coupled-cluster CCSD(T)/cc-pVDZ and CCSD(T)/cc-pVTZ single point calculations [28]. In this work the HF-extrapolated energies were refined using cc-pVQZ, cc-pV5Z and cc-pV6Z basis sets. It was found that the extrapolated HF energy using these extended basis sets did not differ from the *absolute* HF/cc-pV6Z energy by  $>0.3\text{ kJ mol}^{-1}$ . This observation demonstrates that the extrapolation can only slightly improve the HF energy beyond the cc-pV6Z basis set: the HF limit is practically achieved. Similarly, the CCSD(T) correlation energy limit was also updated using CCSD(T)/cc-pVTZ and CCSD(T)/cc-pVQZ single point energies (CCSD(T)/cc-pV(T, Q)Z//MP2/aug-cc-pVDZ). Furthermore, based on MP2/aug-cc-pVDZ geometries, the reaction energy profile was also computed using Weizmann-1 protocol [29] (W1U//MP2/aug-cc-pVDZ) to assess the importance of relativistic effect, core-valence, and empirical corrections. It has turned out that the *relative* energies from W1U//MP2/aug-cc-pVDZ and CCSD(T)/cc-pV(T, Q)Z//MP2/aug-cc-pVDZ levels of theory agree extremely well (within  $1.4\text{ kJ mol}^{-1}$ ), therefore only the CCSD(T)/cc-pV(T, Q)Z//MP2/aug-cc-pVDZ results are discussed in detail.

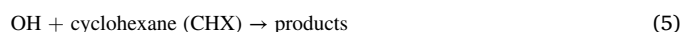
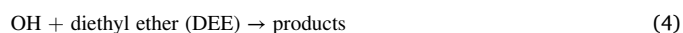
For the transition states, the CCSD(T)/cc-pV(T, Q)Z//MP2/aug-cc-pVDZ zero-point corrected relative energies are within  $1.1\text{ kJ mol}^{-1}$  compared to the previously published CCSD(T)/cc-pV(D, T)Z//MP2/aug-cc-pVDZ values [14] demonstrating high method independency of the results. However, the post-reaction complexes (PC-x) and the THF-R3 radical showed larger method dependency ( $\sim 3.9\text{ kJ mol}^{-1}$ ).

The resulting CCSD(T)/cc-pV(T, Q)Z//MP2/aug-cc-pVDZ energies for the three isotopologues were compiled in Table S4 in the SI and used without any adjustment in the Conventional Transition State Theory (CTST) [30] calculations of the absolute rate coefficients in the temperature range of  $T = 260\text{--}360\text{ K}$ . Similarly to the work of Bansch *et al.* [31], the overall rate coefficients were simply calculated as a sum of all the channel specific rate coefficients by assuming equilibrium between the bimolecular reactants and the pre-reaction complexes (either hydrogen bonded, RC(HB) or van der Waals, RC(vdW) complexes).

## 3. Results and discussion

### 3.1. Experimental rate coefficients

Rate coefficient ratios were determined in the kinetic experiments relative to the reference reactions, (4) or (5):



The main advantage of selecting these reactions as references is that their rate coefficients are well established [8,32] and are of comparable magnitude with those of the targeted reactions (1)–(3).

In case of the reaction  $\text{OH} + \text{THF}$  (1), the following standard relative rate expressions, Eqs. (I) and (II), can be derived:

$$\ln([\text{THF}]_0 / [\text{THF}]_t) = (k_1 / k_4) \times \ln([\text{DEE}]_0 / [\text{DEE}]_t) \quad (I)$$

$$\ln([\text{THF}]_0 / [\text{THF}]_t) = (k_1 / k_5) \times \ln([\text{CHX}]_0 / [\text{CHX}]_t) \quad (\text{II})$$

where [THF], [DEE] and [CHX] stand for the concentrations of tetrahydrofuran, diethyl ether and cyclohexane, respectively, and subscript 0 and subscript t designate concentrations at zero reaction time and subsequent reaction time, respectively. Temperature dependent experiments were performed by using both the OH + DEE (4) and OH + CHX (5) reference reactions.

The RR plots for the reaction of OH with THF according to Eq. (I) are presented at the reaction temperatures  $T = 260, 276, 285, 298, 320, 340$  and  $360$  K in Fig. 1. Linear least-squares analysis of the data of  $\ln([\text{THF}]_0 / [\text{THF}]_t)$  against  $\ln([\text{DEE}]_0 / [\text{DEE}]_t)$  have returned  $k_1 / k_4$  ratios at the 7 reaction temperatures studied. Similar RR straight lines could be obtained for the OH reactions of THF isotopologues (reactions (2) and (3)), from which the rate coefficient ratios ( $k_2 / k_4$ ) and ( $k_3 / k_4$ ) were derived, the corresponding plots are shown in Figures S1 and S2 in the SI.

The RR plots obtained with the OH + CHX (5) reference reaction at the same reaction temperatures as above are presented in Figures S3, S4 and S5 in the SI. The well obeyed straight lines have supplied the rate coefficient ratios  $k_1 / k_5, k_2 / k_5$  and  $k_3 / k_5$ .

All the rate coefficient ratios determined with the OH + DEE (4) and OH + CHX (5) reference reactions are given in Table 1. The ratios were transformed into absolute rate coefficients  $k_i$  ( $i = 1, 2, 3$ ) (Table 1) using the kinetic parameters of the reference reactions OH + DEE (4) and OH + CHX (5) critically evaluated by Calvert et al. [8] and Atkinson [32], respectively; errors were propagated in the calculations.

The rate coefficients determined in the  $T = 260\text{--}360$  K temperature range with two different reference reactions agree reasonably well, their average absolute deviations are 11%, 10% and 9% for the reactions OH + THF (1), OH + THF-d<sub>4</sub> (2) and OH + THF-d<sub>8</sub> (3), respectively. Therefore, in the absence of other information, their averages are proposed as the final rate coefficient values (Table S2). The following rate coefficients are proposed at room temperature:

$$k_1 (\text{OH} + \text{THF}, 298 \text{ K}) = (17.3 \pm 2.3) \times 10^{-12} \text{ cm}^3 \text{ molecule}^{-1} \text{ s}^{-1}$$

$$k_2 (\text{OH} + \text{THF-d}_4, 298 \text{ K}) = (8.50 \pm 1.1) \times 10^{-12} \text{ cm}^3 \text{ molecule}^{-1} \text{ s}^{-1}$$

$$k_3 (\text{OH} + \text{THF-d}_8, 298 \text{ K}) = (8.10 \pm 1.2) \times 10^{-12} \text{ cm}^3 \text{ molecule}^{-1} \text{ s}^{-1}$$

The recommended  $k_1$  (298 K) is in excellent agreement with the average of the literature determinations, which is  $(17.2 \pm 1.5) \times 10^{-12} \text{ cm}^3 \text{ molecule}^{-1} \text{ s}^{-1}$  [10–12]. The  $k_1$  value we propose agrees also within experimental uncertainty with the rate coefficient of the reaction of OD radical with THF,  $k$  (OD + THF, 298 K) =  $(18.1 \pm 2.7) \times 10^{-12} \text{ cm}^3$

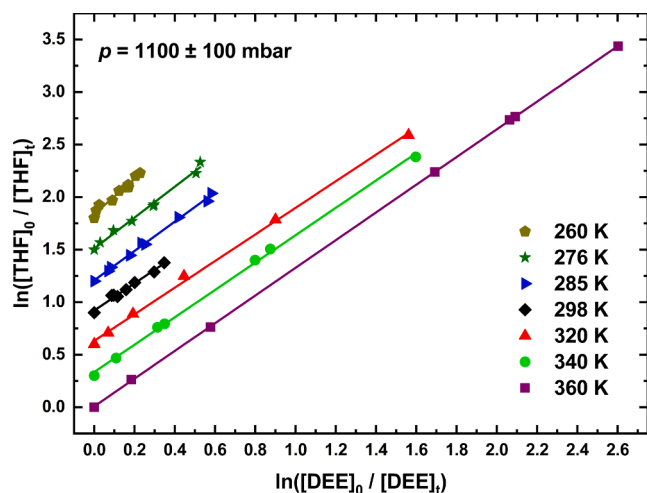


Fig. 1. Relative rate plots used to determine the rate coefficient ratio  $k_1 / k_4$  at different reaction temperatures using the OH + DEE (4) reaction as reference. The experimental data were fitted by Eq. (I), but the  $\ln([\text{THF}]_0 / [\text{THF}]_t)$  data are shifted for each temperature (at  $T < 360$  K) by + 0.3 unit for a better visualization.

Table 1

Kinetic results of the reactions OH + THF (1), OH + THF-d<sub>4</sub> (2) and OH + THF-d<sub>8</sub> (3) determined from RR experiments using OH + DEE (4) and OH + CHX (5) as reference reactions. The rate coefficients  $k_1\text{--}k_5$  are given in  $10^{-11} \text{ cm}^3 \text{ molecule}^{-1} \text{ s}^{-1}$ .

Reaction (i)	T (K)	Reference reaction: OH + DEE (4)			Reference reaction: OH + CHX (5)		
		$(k_i/k_4) \pm 2\sigma$	$(k_4 \pm 2\sigma)^a$	$(k_i \pm 2\sigma)$	$(k_i/k_5) \pm 2\sigma$	$(k_5 \pm 2\sigma)^b$	$(k_i \pm 2\sigma)$
OH + THF (1)	260	1.67 ± 0.12	1.35 ± 0.27	2.26 ± 0.48	4.15 ± {7}	0.60 ± 0.12	2.51 ± 0.60
		{10}^c	0.27	0.48	{7}^c	0.12	0.60
	276	1.47 ± 0.12{8}	1.29 ± 0.26	1.90 ± 0.41	3.59 ± {7}	0.64 ± 0.13	2.31 ± 0.58
					0.56 ± {7}	± 0.13	± 0.58
	285	1.40 ± 0.06{9}	1.27 ± 0.25	1.77 ± 0.36	2.83 ± {7}	0.66 ± 0.13	1.88 ± 0.39
					0.12 ± {7}	± 0.13	± 0.39
	298	1.29 ± 0.07{8}	1.22 ± 0.18	1.58 ± 0.25	2.70 ± {7}	0.70 ± 0.14	1.88 ± 0.39
					0.08 ± {7}	± 0.14	± 0.39
	320	1.27 ± 0.02{6}	1.20 ± 0.24	1.53 ± 0.31	2.24 ± {7}	0.76 ± 0.15	1.69 ± 0.34
					0.05 ± {7}	± 0.15	± 0.34
	340	1.30 ± 0.04{8}	1.18 ± 0.24	1.54 ± 0.31	2.04 ± {7}	0.81 ± 0.16	1.66 ± 0.35
					0.11 ± {7}	± 0.16	± 0.35
	360	1.32 ± 0.02{8}	1.17 ± 0.26	1.55 ± 0.31	1.83 ± {7}	0.88 ± 0.18	1.60 ± 0.34
					0.11 ± {7}	± 0.18	± 0.34
OH + THF-d <sub>4</sub> (2)	260	0.74 ± 0.07	1.35 ± 0.27	1.01 ± 0.22	2.19 ± {7}	0.60 ± 0.12	1.32 ± 0.28
		{11}	0.27	0.22	{7}	0.12	0.28
	276	0.73 ± 0.07{7}	1.29 ± 0.26	0.94 ± 0.12	1.47 ± {7}	0.64 ± 0.13	0.95 ± 0.19
					0.03 ± {7}	± 0.13	± 0.19
	285	0.72 ± 0.01{7}	1.27 ± 0.25	0.90 ± 0.18	1.39 ± {7}	0.66 ± 0.13	0.92 ± 0.19
					0.02 ± {7}	± 0.13	± 0.19
	298	0.66 ± 0.01{9}	1.22 ± 0.18	0.80 ± 0.12	1.28 ± {7}	0.70 ± 0.14	0.89 ± 0.18
					0.03 ± {7}	± 0.14	± 0.18
	320	0.67 ± 0.01{8}	1.20 ± 0.24	0.81 ± 0.16	1.16 ± {7}	0.76 ± 0.15	0.88 ± 0.18
					0.02 ± {7}	± 0.15	± 0.18
	340	0.67 ± 0.01{8}	1.18 ± 0.24	0.79 ± 0.16	1.06 ± {7}	0.81 ± 0.16	0.86 ± 0.17
					0.01 ± {7}	± 0.16	± 0.17
	360	0.66 ± 0.01{8}	1.17 ± 0.26	0.77 ± 0.16	0.98 ± {7}	0.88 ± 0.18	0.86 ± 0.17
					0.02 ± {7}	± 0.18	± 0.17
OH + THF-d <sub>8</sub> (3)	260	0.76 ± 0.08{5}	1.35 ± 0.27	1.03 ± 0.23	1.66 ± {7}	0.60 ± 0.12	1.00 ± 0.22
					0.14 ± {7}	± 0.12	± 0.22
	276	0.68 ± 0.09{6}	1.29 ± 0.26	0.88 ± 0.21	1.47 ± {7}	0.64 ± 0.13	0.94 ± 0.19
					0.02 ± {7}	± 0.13	± 0.19
	285	0.63 ± 0.01{8}	1.27 ± 0.25	0.79 ± 0.16	1.39 ± {7}	0.66 ± 0.13	0.92 ± 0.19
					0.02 ± {7}	± 0.13	± 0.19
	298	0.62 ± 0.08	1.22 ± 0.18	0.75 ± 0.14	1.24 ± {7}	0.70 ± 0.14	0.87 ± 0.18
		{10}	0.18	0.14	{7}	0.14	0.18
	320	0.61 ± 0.03{8}	1.20 ± 0.24	0.73 ± 0.15	1.07 ± {7}	0.76 ± 0.15	0.81 ± 0.16
					0.01 ± {7}	± 0.15	± 0.16
	340	0.61 ± 0.02	1.18 ± 0.24	0.72 ± 0.15	0.97 ± {7}	0.81 ± 0.16	0.79 ± 0.16
		{7}	0.24	0.15	{7}	0.16	0.16
	360	0.65 ± 0.01{7}	1.17 ± 0.26	0.76 ± 0.15	0.91 ± {7}	0.88 ± 0.18	0.80 ± 0.16
					0.01 ± {7}	± 0.18	± 0.16

<sup>a</sup> Rate coefficient of the reference reaction taken from [8]. <sup>b</sup> Rate coefficient of the reference reaction taken from [32]. <sup>c</sup> The number of RR data points are given in curly brackets.

molecule<sup>-1</sup> s<sup>-1</sup> [9], as anticipated by the very similar reactivity of OH and OD [33].

The rate coefficient of the reaction of OH radical with THF is a high value compared with those of OH + cyclobutane and OH + cyclopentane reactions [32] indicating a rate enhancing effect of the ether group in the THF molecule. This effect is somewhat less significant, however, than that observed for aliphatic ethers which may be taken as an indication for that the ring structure reduces the range of action of the activating effect [34].

To the best of our knowledge, no kinetic information is available for the reactions of OH with deuterated tetrahydrofurans. The rate coefficients determined and presented in Table 1 reveal a normal kinetic isotope effect (KIE) for both the OH + THF-d<sub>4</sub> (2) and OH + THF-d<sub>8</sub> (3) reactions; the KIE ratios are  $k_1/k_2 = 2.04 \pm 0.38$  and  $k_1/k_3 = 2.14 \pm 0.43$  at room temperature. These values are similar to the KIEs of the abstraction of secondary C–H/D-atoms by OH radicals both from acyclic and cyclic hydrocarbons ( $k_H/k_D \approx 2$ ) [33].

A two-parameter Arrhenius expression was used to describe the temperature dependences of the experimental rate coefficients in the temperature range  $T = 260$ – $360$  K. Non-linear least-squares fits resulted in the following rate coefficient expressions (the respective  $\ln k_i$  vs.  $1/T$  linearized plots are presented in Fig. 2, where  $i = 1, 2$  or 3):

$$k_1 = (5.7 \pm 3.2) \times 10^{-12} \exp [(2.9 \pm 1.4 \text{ kJ mol}^{-1}) / RT] \text{ cm}^3 \text{ molecule}^{-1} \text{ s}^{-1}$$

$$k_2 = (3.8 \pm 1.9) \times 10^{-12} \exp [(2.2 \pm 1.2 \text{ kJ mol}^{-1}) / RT] \text{ cm}^3 \text{ molecule}^{-1} \text{ s}^{-1}$$

$$k_3 = (3.7 \pm 1.3) \times 10^{-12} \exp [(2.1 \pm 0.9 \text{ kJ mol}^{-1}) / RT] \text{ cm}^3 \text{ molecule}^{-1} \text{ s}^{-1}$$

The overall rate coefficients of the two different deuterated THF isotopologues agree within a few percent which can be interpreted as the H-abstraction from  $\beta$ -position has no kinetic relevance in the temperature range studied.

Rate coefficients published in the literature for the reaction OH + THF (1) [10–13] together with our own determinations are presented in Arrhenius representation in Fig. 3. As seen, the negative temperature dependence reported by Moriarty *et al.* [12] has been confirmed by our study, although the effect is very small and the kinetic data are burdened with substantial uncertainty. On the other hand, however, the rate coefficients we report at the respective temperatures agree within 10% of the published data.

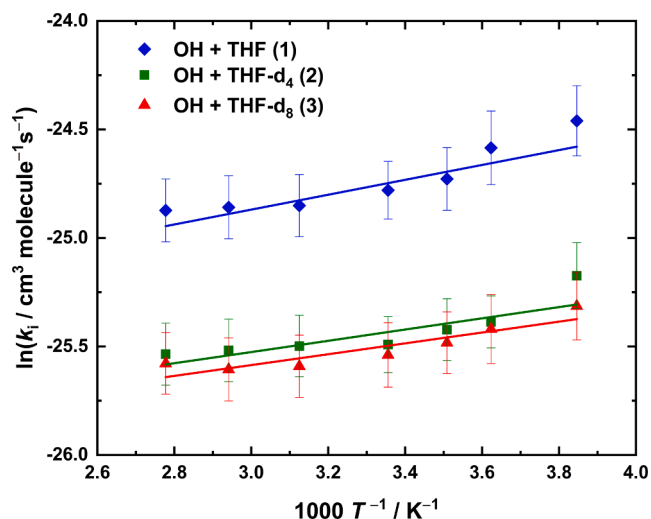


Fig. 2.  $\ln k_i$  vs.  $1/T$  Arrhenius plots ( $i = 1, 2, 3$ ) of the experimentally determined rate coefficients of the reactions OH + THF (1), OH + THF-d<sub>4</sub> (2) and OH + THF-d<sub>8</sub> (3) and the best fit results obtained by non-linear least squares analysis.

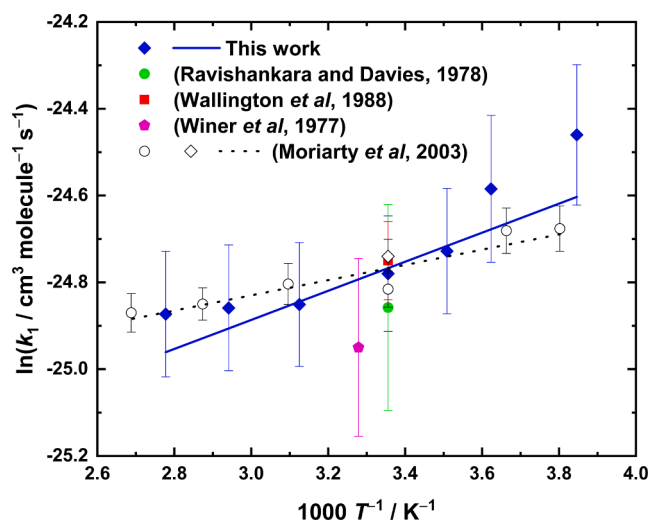


Fig. 3. Arrhenius plot for the temperature dependence of the rate coefficient for the reaction OH + THF (1) determined in current experiments and reported in the literature over the temperature range  $T = 260$ – $372$  K.

### 3.2. Theoretical results

The OH + THF reaction system had been discussed in detail by Giri *et al.* [14]. Here we report quantum chemical results and computed rate coefficients for the reactions of OH radical with THF, THF-d<sub>4</sub> and THF-d<sub>8</sub> for the first time concerning the deuterated tetrahydrofuran reactions. The reaction mechanisms and molecular structures, including those of the deuterated species, have been found very similar to those reported in [14]. Therefore, energetics of the transition states (TSs) and molecular complexes (RCs and PCs) formed on along the reaction pathways are discussed in more detail in the present paper.

The quantum chemical computations were performed at the CCSD (T)/cc-pV(T,Q)Z//MP2/aug-cc-pVDZ level of theory, a potential energy diagram is shown in Fig. 4. Cartesian coordinates and molecular structures for the reaction system OH + THF have been presented in Table S3 and Figure S6 in the SI; all the computed relative energies are summarised in Table S4.

As presented in Fig. 4, the zero-point corrected relative energies for the transition states (TSs) increased by 3.3–4.3 kJ mol<sup>-1</sup> upon perdeuteration, although no significant isotope effect was found in the relative energy of both pre-reaction complexes (RCs) of the OH + THF reaction (RC(vdW) stands for van der Waals complex of THF and OH radical, while RC(HB) is its hydrogen bonded counterpart). The relative energies of the post-reaction complexes (noted as PCs) increased only slightly (0.9–2.3 kJ mol<sup>-1</sup>). Similarly to the perdeuteration, tetradeuteration (reaction OH + THF-d<sub>4</sub>) has also increased the relative energies of the transition states, TS-2A and TS-2B by 3.4–3.5 kJ mol<sup>-1</sup>, but those of TS-3A, TS-3B and TS-3C are not affected.

As reported previously [14], the hydrogen abstraction of THF at the  $\beta$ -position by OH is the major reaction channel above 1200 K, but it is of minor significance at temperatures of the current experiments, and therefore the H-abstraction from various  $\alpha$ -sites of THF leading to the formation of tetrahydrofuran-2-yl radical (THF-R2) is dominant over the entire temperature range studied here. This is also in line with the present CTST calculations: the reaction channels leading to the formation of the product radical tetrahydrofuran-3-yl (THF-R3) through TS-3A, TS-3B and TS-3C contribute negligibly to the overall rate (<0.1%) in the temperature range studied. It is also worth noting that the energy profile of the relevant reaction channels has similar characteristics to that of the OH + dimethyl ether reaction [31]: a submerged TS (with  $-3.35$  kJ mol<sup>-1</sup> – see Figure 6 of Bänisch *et al.* [31]) correlates with a pre-reaction complex which lies  $\sim 20$  kJ mol<sup>-1</sup> below reactants. For such a case it was shown that CTST rate coefficients can reproduce

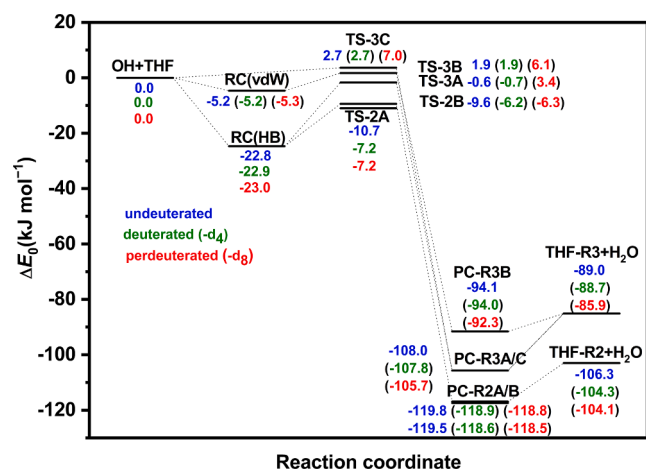


Fig. 4. Zero-point corrected CCSD(T)/cc-pV(T,Q)Z//MP2/aug-cc-pVDZ potential energies ( $\Delta E_0$ ) for the reactions OH + THF (1), OH + THF- $d_4$  (2) and OH + THF- $d_8$  (3); energies are relative to reactant energies.

RC(vdW): pre-reaction van der Waals complex; RC(HB): pre-reaction hydrogen bonded complex; TS-2A and TS-2B: transition states leading to the formation of the tetrahydrofuran-2-yl (THF-R2) radical, TS-3A, TS-3B and TS-3C: transition states leading to the formation of the tetrahydrofuran-3-yl (THF-R3) radical; PC-R2A and PC-R2B: post-reaction complexes of THF-R2 with H<sub>2</sub>O, formed through TS-2A and TS-2B, respectively; PC-R3A, PC-R3B and PC-R3C: post-reaction complexes of THF-R3 with H<sub>2</sub>O, formed through TS-3A, TS-3B and TS-3C, respectively.

experimental ones remarkably well [31,35]. The temperature dependences of the computed rate coefficients can be described by the following three-parameter Arrhenius expression:

$$k(T) = A \times (T / 298.15 \text{ K})^n \times e^{-E / (R T)} \text{ cm}^3 \text{ molecule}^{-1} \text{ s}^{-1} \quad (\text{III})$$

The calculated data were fitted to Eq. (III) by using a non-linear least squares procedure to obtain the generalized Arrhenius parameters which are tabulated in Table 2. It is a common practice in CTST to correct the calculated rate coefficients by the Wigner tunnelling factor [30]. No such correction in our present study has been made, however, because of the recognized tendency of overcorrection of tunnelling.

### 3.3. Evaluation of standard enthalpies of formation

Results of our quantum chemical computations performed at the high theoretical levels of W1U//MP2/aug-cc-pVDZ and CCSD(T)/cc-pV(T,Q)Z//MP2/aug-cc-pVDZ allowed the determination of new gas-phase standard enthalpies of formation at 0 K ( $\Delta_f H^\circ_0$ ) and 298.15 K ( $\Delta_f H^\circ_{298}$ ) for the THF molecule, THF-R2 and THF-R3 radicals using atomization scheme (AS) and isodesmic reaction (IR) protocols. (The corresponding set of IR reactions are presented in Figure S7 in the SI.) We have applied the coupled cluster theory by taking into account also the effect of perturbative triples at calculating the electronic energies and the basis set we used included diffuse functions as well (see also [36;37]). The derived enthalpies of formation are presented in Table 3 along with data from the literature.

As Table 3 shows, the experimental value of the standard enthalpy of formation of THF derived from flame calorimetry measurements by Pell

Table 2

Arrhenius parameters for the high-pressure limiting values of the total rate coefficients calculated from CTST for  $T = 260\text{--}360 \text{ K}$ .

Reaction	$A$ ( $\text{cm}^3 \text{ molecule}^{-1} \text{ s}^{-1}$ )	$n$	$E / R$ (K)
OH + THF (1)	$8.2 \times 10^{-16}$	9.1	3212
OH + THF- $d_4$ (2)	$5.8 \times 10^{-14}$	2.9	1412
OH + THF- $d_8$ (3)	$3.3 \times 10^{-15}$	6.8	2306

Table 3

Standard gas-phase enthalpies of formation obtained from CCSD(T)/cc-pV(T,Q)Z//MP2/aug-cc-pVDZ and W1U//MP2/aug-cc-pVDZ computations and comparison with literature.

Name	$\Delta_f H^\circ_0$ (kJ mol <sup>-1</sup> )	$\Delta_f H^\circ_{298}$ (kJ mol <sup>-1</sup> )	Notes
Tetrahydrofuran (THF)	-153.9	-178.6	This work (CCSD(T)/cc-pV(T,Q)Z//MP2/aug-cc-pVDZ) <sup>a</sup>
	-159.4 ± 1.6	-186.3 ± 1.0	This work (CCSD(T)/cc-pV(T,Q)Z//MP2/aug-cc-pVDZ) <sup>b</sup>
	-157.7 ± 0.8	-184.5 ± 0.8	This work (W1U//MP2/aug-cc-pVDZ) <sup>b</sup>
	-155.5 ± 8	-182.5 ± 8.0	Pell & Pilcher (flame calorimetry) [38]
	-157.3 ± 2.9	-184.2 ± 2.1	Goos et al. (G3B3) <sup>a</sup> [44]
	-158.6 ± 0.9	-185.4 ± 0.6	Feller & Franz (CBS(FC)/DTQ) <sup>a</sup> [36]
	-157.3 ± 2.9	-184.1 ± 2.1	Auzmendi-Murua & Bozzelli (CBS-QB3, G3MP2B3) <sup>b</sup> [45]
	-158.6 ± 18.0	-185.4 ± 0.6	This work (average of IR determinations)
Tetrahydrofuran-2-yl radical (THF-R2)	18.0	-2.9	This work (CCSD(T)/cc-pV(T,Q)Z//MP2/aug-cc-pVDZ) <sup>a</sup>
	8.4 ± 1.1	-14.3 ± 1.2	This work (CCSD(T)/cc-pV(T,Q)Z) <sup>b</sup>
	9.5 ± 1.9	-13.2 ± 2.0	This work (W1U//MP2/aug-cc-pVDZ) <sup>b</sup>
	21.3 ± 4.2	-2.1 ± 4.2	Feller & Franz (CBS(FC)/DTQ) <sup>a</sup> [36]
		-11.3 ± 1.2	Simmie(CBS-QB3, G3,CBS-APNO) <sup>b</sup> [37]
		-8.5 ± 3.6	Auzmendi-Murua & Bozzelli (CBS-QB3, G3MP2B3) <sup>b</sup> [45]
	9.0 ± 1.1	-13.8 ± 1.2	This work (average of IR determinations)
Tetrahydrofuran-3-yl radical (THF-R3)	35.3	15.5	This work (CCSD(T)/cc-pV(T,Q)Z) <sup>a</sup>
	25.7 ± 1.1	4.2 ± 1.2	This work (CCSD(T)/cc-pV(T,Q)Z) <sup>b</sup>
	27.3 ± 1.9	5.7 ± 2.0	This work (W1U//MP2/aug-cc-pVDZ) <sup>b</sup>
	37.2 ± 4.2	15.1 ± 4.2	Feller & Franz (CBS(FC)/DTQ) <sup>a</sup> [36]
		7.9 ± 1.5	Simmie(CBS-QB3, G3,CBS-APNO) <sup>b</sup> [37]
		10.5 ± 3.6	Auzmendi-Murua & Bozzelli (CBS-QB3, G3MP2B3) <sup>b</sup> [45]
	26.5 ± 1.1	5.0 ± 1.2	This work (average of IR determinations)

<sup>a</sup> Obtained by atomization approach (AS). <sup>b</sup>Using isodesmic work reactions (IR).

and Pilcher [38] is more exothermic by 5.6 kJ mol<sup>-1</sup> than our AS result, while the IR scheme has provided excellent agreement with the calorimetric data (within 2.1 kJ mol<sup>-1</sup> for CCSD(T) and 0.3 kJ mol<sup>-1</sup> for W1U computation). The observed inferior performance of AS when applying even high level quantum chemical methods is surprising in view of recent benchmarking studies of enthalpies of formation derived by the atomization approach (see e.g. [39]) and may be due to fortuitous accumulation of small computational errors.

Concerning THF radicals, the literature data are less consistent, our IR results are in line with more exothermic values reported by Simmie et al. [37] for both the THF-R2 and THF-R3 radicals (the deviation is <3 kJ mol<sup>-1</sup>). Most of the computational results reported in the literature were obtained by using variants of composite quantum chemical methods (Table 3) which apply empirically adjusted parameters such as the Complete Basis Set (CBS) family of methods developed by Petersson

and co-workers ([40,41]) and the Gaussian-3 (G3) methods ([42,43]). Beside these, Feller and Franz computed the THF radicals by using their non-parametrized composite coupled cluster method [36] with application of the atomization approach. They have reported  $\Delta_f H^\circ$  values which agree well with our AS data, but differ substantially from those obtained by the application of parametrized quantum chemical methods and our determinations applying isodesmic reaction scheme (Table 3). It appears therefore that the computed enthalpy of formation is more sensitive to the derivation method rather than the level of quantum chemical theory used.

Considering all information available, we propose for the enthalpies of formation of THF and the THF radicals the average values from our current study that were determined by using isodesmic reaction schemes: these are listed also in Table 3. The proposed standard enthalpies of formation correspond to the bond dissociation enthalpies of  $DH^\circ_0(\text{THF-R2-H}) = 383.6$  and  $DH^\circ_0(\text{THF-R3-H}) = 401.1$  as well as to  $DH^\circ_{298}(\text{THF-R2-H}) = 389.6$  and  $DH^\circ_{298}(\text{THF-R3-H}) = 408.4$  kJ mol<sup>-1</sup>.

### 3.4. Comparison of experiment and theory

The experimental and theoretical rate coefficients we have determined in our current work are compared in the form of Arrhenius plots in Fig. 5.

As seen in Fig. 5, both experiment and theory predict small, but definite negative temperature dependences for the studied OH reactions over the temperature range of  $T = 260\text{--}360$  K. CCSD(T)/cc-pV(T,Q)Z//MP2/aug-cc-pVDZ based estimations of the high-pressure limit rate coefficients by CTST are in excellent agreement for the reaction OH + THF-d<sub>8</sub> (3) (agree within 5%), agree reasonably well for OH + THF-d<sub>4</sub> (2) (within 35%), while such calculations overestimate the rate coefficient of the OH + THF (1) reaction by a factor of  $\sim 1.5$ . Deviation from experiment may be due to approximations used in CTST, such as the neglect of re-crossing of trajectories at the transition state that gives rise to overestimation of the theoretical rate coefficients and the harmonic approximation in treating molecular vibrations [46,47].

The small difference between the rate coefficients for OH + THF-d<sub>4</sub> (2) and OH + THF-d<sub>8</sub> (3) indicates that H/D isotope substitution at the  $\beta$ -position has negligible kinetic effect, suggesting that H-abstraction from  $\beta$ -position must be a minor channel in the temperature range studied. This conclusion is in line with that the bond dissociation energy of the  $\beta$ -C-H bond is higher by  $\sim 19$  kJ mol<sup>-1</sup> compared with that of the  $\alpha$ -C-H bond in the THF molecule (Section 3.3.).

The experimentally determined primary KIEs ( $k_1/k_2$  and  $k_1/k_3$ ) are close to 2, and vary little with temperature. Computations have returned significantly higher values: the average KIEs being  $k_1/k_2 \approx 6.2$  and  $k_1/k_3 \approx 5.2$  over the temperature range of  $T = 260\text{--}360$  K. As presented in the previous paragraph, the computed  $k_1$  appears to be an overestimate which may explain the higher KIEs from theory compared with experiment. It is noted also that the KIEs computed by CTST have been reported substantially higher than the experimental values for several other reactions as well, see, e.g. [46,48,49] which point once again to problems associated with the approximations used in CTST including multidimensional quantum effects and the harmonic approximation in treating the vibrational modes [47,50].

## 4. Conclusion

The relative rate kinetic method was used to determine rate coefficients ( $k_i$ ,  $i = 1, 2, 3$ ) for the overall reactions of OH radicals with tetrahydrofuran (1), 2,2,5,5-tetradeutero-tetrahydrofuran (2) and perdeuterated tetrahydrofuran (3) over the temperature range of  $T = 260\text{--}360$  K at  $p = 1100$  mbar pressure.  $k_1$  has been found  $\sim 2$ -times higher than both  $k_2$  and  $k_3$  displaying a normal primary kinetic isotope effect for a H/D abstraction. The rate coefficients  $k_2$  and  $k_3$  are close to each other indicating that H-atoms are abstracted predominantly from the alpha position of the THF molecule by OH at the relatively low

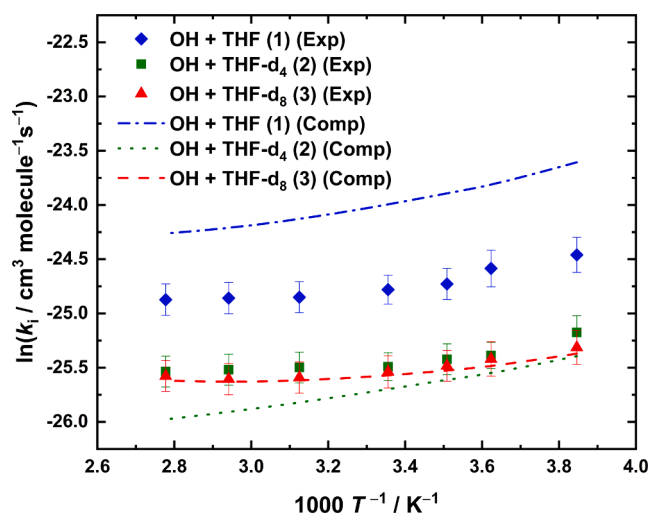


Fig. 5.  $\ln k_i$  vs.  $1/T$  ( $i = 1, 2, 3$ ) Arrhenius plots of experimental and computed rate coefficients for the reactions OH + THF (1), OH + THF-d<sub>4</sub> (2) and OH + THF-d<sub>8</sub> (3) in the temperature range of the experiments,  $T = 260\text{--}360$  K.

temperature of the experiments. All three reactions show small negative temperature dependences in the temperature range studied characterized by an activation energy of  $\sim -2$  kJ mol<sup>-1</sup>. Quantum chemistry computations performed at the CCSD(T)/cc-pV(T,Q)Z//MP2/aug-cc-pVDZ level of theory have revealed the reactions to occur through pre- and postreaction complexes and transition states along the lowest energy reaction paths with maxima that lie below the energy level of the reactants. Kinetics of the reactions could be described reasonably well by conventional transition state theory with the assumption of an equilibrium between the reactants and the prereaction complex using the computed ab initio data as input parameters for the rate theory calculations. The high level quantum chemical results have been used for derivation of enthalpies of formation for THF and the THF radicals, THF-R2 and THF-R3.

### CRedit authorship contribution statement

Ádám Illés: Investigation, Writing - original draft. Zsófia Borbála Rózsa: Investigation. Ravikumar Thangaraj: Investigation. Erzsébet Décsiné Gombos: Investigation. Sándor Dóbbé: Writing - review & editing. Binod Raj Giri: Writing - review & editing. Milán Szóri: Investigation, Writing - original draft.

### Declaration of Competing Interest

The authors declare that they have no known competing financial interests or personal relationships that could have appeared to influence the work reported in this paper.

### Acknowledgements

This work was supported by the National Research, Development and Innovation Office of Hungary (NVKP\_16-2016-1-0045). It was supported also by the EU and the Hungarian State, co-financed by the European Regional Development Fund (GINOP-2.3.4-15-2016-00004 project). M. Sz. gratefully acknowledges the financial support from the János Bolyai Research Scholarship of the Hungarian Academy of Sciences (BO/00113/15/7), and from the New National Excellence Program of the Ministry of Human Capacities (ÚNKP-17-4-III-ME/26). Research reported in this work was also funded by King Abdullah University of Science and Technology (KAUST).

## Appendix A. Supplementary data

Supplementary data to this article can be found online at <https://doi.org/10.1016/j.cplett.2021.138698>.

## References

- [1] L. Karas, W.J. Piel, *Ethers*, Kirk-Othmer Encyclopedia of Chemical Technology, John Wiley & Sons Inc, 2004.
- [2] C. Jin, X. Zhang, Z. Geng, X. Pang, X. Wang, J. Ji, G. Wang, H. Liu, Effects of various co-solvents on the solubility between blends of soybean oil with either methanol or ethanol, *Fuel* 244 (2019) 461–471.
- [3] T.T. Kasper, A. Lucassen, A.W. Jasper, W. Li, P.R. Westmoreland, K. Kohse-Höinghaus, B. Yang, J. Wang, T.A. Cool, N. Hansen, Identification of tetrahydrofuran reaction pathways in premixed flames, *Z. Phys. Chem.* 225 (2011) 1237–1270.
- [4] L.-S. Tran, M. Verdicchio, F. Monge, R.C. Martin, R. Bounaceur, B. Sirjean, P.-A. Glaude, M.U. Alzueta, F. Battin-Leclerc, An experimental and modeling study of the combustion of tetrahydrofuran, *Combust. Flame* 162 (2015) 1899–1918.
- [5] I.O. Antonov, J. Zádor, B. Rotavera, E. Papajak, D.L. Osborn, C.A. Taatjes, L. Sheps, Pressure-dependent competition among reaction pathways from first- and second- $O_2$  additions in the low-temperature oxidation of tetrahydrofuran, *J. Phys. Chem. A* 120 (2016) 6582–6595.
- [6] M. Verdicchio, B. Sirjean, L.S. Tran, P.A. Glaude, F. Battin-Leclerc, Unimolecular decomposition of tetrahydrofuran: Carbene vs. diradical pathways, *Proc. Combust. Inst.* 35 (1) (2015) 533–541.
- [7] Y. Fenard, A. Gil, G. Vanhove, H.-H. Carstensen, K.M. Van Geem, P. R. Westmoreland, O. Herbinet, F. Battin-Leclerc, A model of tetrahydrofuran low-temperature oxidation based on theoretically calculated rate constants, *Combust. Flame* 191 (2018) 252–269.
- [8] J.G. Calvert, A. Mellouki, J. Orlando, M.J. Pilling, T.J. Wallington, *Mechanism of Atmospheric Oxidation of the Oxygenates*, Oxford University Press, New York, 2011.
- [9] C. Andersen, O.J. Nielsen, F.F. Østerstrøm, S. Ausmeel, E.J.K. Nilsson, M.P. S. Andersen, Atmospheric Chemistry of Tetrahydrofuran, 2-Methyltetrahydrofuran, and 2,5-Dimethyltetrahydrofuran: Kinetics of Reactions with Chlorine Atoms, OD Radicals, and Ozone, *J. Phys. Chem. A* 120 (2016) 7320–7326.
- [10] A.R. Ravishankara, D.D. Davis, Kinetic Rate Constants for the Reaction of OH with Methanol, Ethanol, and Tetrahydrofuran at 298 K, *J. Phys. Chem.* 82 (1978) 2852–2853.
- [11] T.J. Wallington, R. Liu, P. Dagaut, M.J. Kurylo, The gas phase reactions of hydroxyl radicals with a series of aliphatic ethers over the temperature range 240–440 K, *Int. J. Chem. Kinet.* 20 (1988) 41–49.
- [12] J. Moriarty, H. Sidebottom, J. Wenger, A. Mellouki, G. Le Bras, Kinetic studies on the reactions of hydroxyl radicals with cyclic ethers and aliphatic diethers, *J. Phys. Chem. A* 107 (2003) 1499–1505.
- [13] A.M. Winer, A.C. Lloyd, R. Darnall, R. Atkinson, J.N. Pitts Jr., Rate constants for the reaction of OH radicals with n-propyl acetate, sec-butyl acetate, tetrahydrofuran and peroxyacetyl nitrate, *Chem. Phys. Lett.* 51 (1977) 221–226.
- [14] B.R. Giri, F. Khaled, M. Szóri, B. Viskolcz, A. Farooq, An experimental and theoretical kinetic study of the reaction of OH radicals with tetrahydrofuran, *Proc. Combust. Inst.* 36 (2017) 143–150.
- [15] M.J. Kurylo, V.L. Orkin, Determination of atmospheric lifetimes via the measurement of OH radical kinetics, *Chem. Rev.* 103 (2003) 5049–5076.
- [16] T. Brauers, B.J. Finnlaysen-Pitts, Analysis of relative rate measurements, *Int. J. Chem. Kinet.* 29 (1997) 665–672.
- [17] Á. Illés, M. Farkas, G.L. Zügner, G.Y. Novodárszki, M. Mihályi, S. Dóbe, Direct and relative rate coefficients for the gas-phase reaction of OH radicals with methyltetrahydrofuran at room temperature, *Reac. Kinet. Mech. Cat.* 119 (2016) 5–18.
- [18] W.D. Taylor, T.D. Allston, M.J. Moscato, G.B. Fazekas, R. Kozłowski, G.A. Takacs, Atmospheric photo-dissociation lifetimes for nitromethane, methyl nitrite, and methyl nitrate, *Int. J. Chem. Kinet.* 12 (1980) 231–240.
- [19] F. Khaled, B.R. Giri, M. Szóri, T.V.-T. Mai, L.K. Huynh, A. Farooq, A combined high-temperature experimental and theoretical kinetic study of the reaction of dimethyl carbonate with OH radicals, *Phys. Chem. Chem. Phys.* 19 (2017) 7147–7157.
- [20] M. AlAbbad, B.R. Giri, M. Szóri, A. Farooq, On the high-temperature unimolecular decomposition of ethyl levulinate, *Proc. Combust. Inst.* 36 (2017) 187–193.
- [21] J.P. Merrick, D. Moran, L. Radom, An Evaluation of Harmonic Vibrational Frequency Scale Factors, *J. Phys. Chem. A* 111 (2007) 11683–11700.
- [22] C. Møller, M.S. Plesset, Note on an Approximation Treatment for Many-Electron Systems, *Phys. Rev.* 46 (1934) 618–622.
- [23] T.H. Dunning, Gaussian basis sets for use in correlated molecular calculations. I. The atoms boron through neon and hydrogen, *J. Chem. Phys.* 90 (1989) 1007–1023.
- [24] W.J. Hehre, L. Radom, P.v.R. Schleyer, J.A. Pople, *Ab Initio Molecular Orbital Theory*. 1986. John Wiley, New York, 548 pp.
- [25] M.J. Frisch, G.W. Trucks, H.B. Schlegel, et al., *Gaussian 09*, Revision B.01, (Gaussian Inc, Wallingford, CT, 2009).
- [26] D. Feller, Application of systematic sequences of wave functions to the water dimer, *J. Chem. Phys.* 96 (1992) 6104–6114.
- [27] T. Helgaker, W. Klopper, Basis-set convergence of correlated calculations on water, *J. Chem. Phys.* 106 (1997) 9639–9646.
- [28] J.D. Watts, J. Gauss, R.J. Bartlett, Coupled-cluster methods with noniterative triple excitations for restricted open-shell Hartree-Fock and other general single determinant reference functions. Energies and analytical gradients, *J. Chem. Phys.* 98 (1993) 8718–8733.
- [29] J.M.L. Martin, G. de Oliveira, Towards standard methods for benchmark quality ab initio thermochemistry – W1 and W2 theory, *J. Chem. Phys.* 111 (1999) 1843–1856.
- [30] K.J. Laidler, *Chemical Kinetics*. 1987, Harper & Row Publishers, New York, Cambridge, Philadelphia, etc.
- [31] C. Bänisch, J. Kiecherer, M. Szóri, M. Olzmann, Reaction of Dimethyl Ether with Hydroxyl Radicals: Kinetic Isotope Effect and Prereactive Complex Formation, *J. Phys. Chem. A* 117 (2013) 8343–8351.
- [32] R. Atkinson, Kinetics of the gas-phase reactions of OH radicals with alkanes and cycloalkanes, *Atmos. Chem. Phys.* 3 (2003) 2233–2307.
- [33] Roger Atkinson, Kinetics and Mechanism of the Gas-Phase Reactions of the Hydroxyl Radical with Organic Compounds, *J. Phys. Chem. Ref. Data*, Monograph 1 (1989).
- [34] A. Mellouki, G. Le Bras, H. Sidebottom, Kinetics and Mechanisms of the Oxidation of Oxygenated Organic Compounds in the Gas Phase, *Chem. Rev.* 103 (2003) 5077–5096.
- [35] S. Thion, A.M. Zaras, M. Szóri, P. Dagaut, Theoretical kinetic study for methyl levulinate: oxidation by OH and  $CH_3$  radicals and further unimolecular decomposition pathways, *Phys. Chem. Chem. Phys.* 17 (2015) 23384–23391.
- [36] D. Feller, J.A. Franz, A theoretical determination of the heats of formation of furan, tetrahydrofuran, THF-2-yl, and THF-3-yl, *J. Phys. Chem. A* 104 (2000) 9017–9025.
- [37] J.M. Simmie, Kinetics and thermochemistry of 2,5-dimethyltetrahydrofuran and related oxolanes: next next-generation biofuels, *J. Phys. Chem. A* 116 (2012) 4528–4538.
- [38] A.G. Baboul, L.A. Curtiss, P.C. Redfern, K. Raghavachari, Gaussian-3 theory using density functional geometries and zero-point energies, *J. Chem. Phys.* 110 (1999) 7650–7657.
- [39] E. Paulechka, A. Kazakov, Efficient DLPNO–CCSD(T)-Based Estimation of Formation Enthalpies for C-, H-, O-, and N-Containing Closed-Shell Compounds Validated Against Critically Evaluated Experimental Data, *J. Phys. Chem. A* 121 (2017) 4379–4387.
- [40] A. Petersson, M.A. Al-Laham, A complete basis set model chemistry. II. Open-shell systems and the total energies of the first-row atoms, *J. Chem. Phys.* 94 (1991) 6081–6090.
- [41] J.W. Ochterski, G.A. Petersson, J.A. Montgomery Jr., A complete basis set model chemistry. V. Extensions to six or more heavy atoms, *J. Chem. Phys.* 104 (1996) 2598–2619.
- [42] L.A. Curtiss, K. Raghavachari, P.C. Redfern, V. Rassolov, J.A. Pople, Gaussian-3 (G3) theory for molecules containing first and second-row atoms, *J. Chem. Phys.* 109 (1998) 7764–7776.
- [43] A.S. Pell, G. Pilcher, Measurements of heats of combustion by flame calorimetry. Part 3. –Ethylene oxide, trimethylene oxide, tetrahydrofuran and tetrahydropyran, *Trans. Faraday Soc.* 61 (1965) 71–77.
- [44] E. Goos, A. Burcat, B. Ruscic, Extended Third Millennium Ideal Gas and Condensed Phase Thermochemical Database for Combustion with Updates from Active, Thermochemical Tables (2016).
- [45] I. Auzmendi-Murua, J.W. Bozzelli, Thermochemical Properties and Bond Dissociation Enthalpies of 3- to 5-Member Ring Cyclic Ether Hydroperoxides, Alcohols, and Peroxy Radicals: Cyclic Ether Radical +  $^3O_2$  Reaction Thermochemistry, *J. Phys. Chem. A* 118 (2014) 3147–3167.
- [46] W.-P. Hu, I. Rossi, J.C. Corchado, D.G. Truhlar, Molecular Modeling of Combustion Kinetics. The Abstraction of Primary and Secondary Hydrogens by Hydroxyl Radical, *J. Phys. Chem. A* 101 (1997) 6911–6921.
- [47] L. Jun, H. Guo, Thermal Rate Coefficients and Kinetic Isotope Effects for the Reaction  $OH + CH_4 \rightarrow H_2O + CH_3$  on an ab Initio-Based Potential Energy Surface, *J. Phys. Chem. A* 122 (2018) 2645–2652.
- [48] A.R. Ravishankara, J.M. Nicovich, R.L. Thompson, F.P. Tully, Kinetic Study of the Reaction of OH with  $H_2$  and  $D_2$  from 250 to 1050 K, *J. Phys. Chem.* 85 (1981) 2498–2503.
- [49] T. Gierczak, R.K. Talukdar, S.C. Herndon, G.L. Vaghjiani, A.R. Ravishankara, Rate Coefficients for the Reactions of Hydroxyl Radicals with Methane and Deuterated Methanes, *J. Phys. Chem. A* 101 (1997) 3125–3134.
- [50] Á. González-Lafont, J.M. Lluch, Kinetic isotope effects in chemical and biochemical reactions: physical basis and theoretical methods of calculation, *WIREs Comput. Mol. Sci.* 6 (2016) 584–603.